Artificial Horseshoe Orbits Using Low Thrust Propulsion

Callum S. Arnot[a], Colin R. McInnes[b]

[a] *PhD candidate, Advanced Space Concepts Laboratory, Department of Mechanical and Aerospace Engineering, University of Strathclyde*, callum.arnot@strath.ac.uk
[b] *James Watt Chair, Professor of Engineering Science, School of Engineering, University of Glasgow*, colin.mcinnes@glasgow.ac.uk

Abstract

Horseshoe orbits, occurring naturally in three-body systems, can be generated artificially in a two-body system with the application of continuous low thrust. In this paper, the Clohessy-Wiltshire equations are presented in cylindrical polar form, and with the addition of continuous low thrust they are used to generate artificial horseshoe orbits around a circular reference orbit. Two solutions using simple thrust commands are derived and tested numerically. It is shown that the thrust magnitude and Δv requirements for artificial horseshoe orbits are modest and achievable for certain Earth orbiting cases, and that the applications for such novel spacecraft constellations are potentially diverse. Finally, a discussion of phased constellations of spacecraft, considering constellations on nested horseshoe orbits around the same reference orbit and those on displaced-plane non-Keplerian orbits, is also presented.
Keywords: Low thrust, horseshoe orbits, formation flying, non-Keplerian orbits

1. Introduction

The existence of co-orbital resonant motion has been acknowledged and studied for over a century by many authors, due to the existence of the Trojan asteroids which follow relative trajectories around either of the two triangular Lagrange points in the Sun-Jupiter gravitational system. Because these objects offered the only real examples of this motion, work mainly considered the 'tadpole' orbits (around a single triangular Lagrange point) that these followed. However, in 1980-1981, the Voyager mission observed two co-orbiting satellites of Saturn, namely Janus and Epimethus [1, 2, 3], which followed relative trajectories encompassing the three Lagrange points (L_3, L_4, and L_5) of that system. Thus, confirmation had been attained that 'horseshoe' orbits existed, which had previously been classified within the restricted three-body problem (RTBP) by Garfinkel in 1977 [4] but which had been only considered in a theoretical sense.

More recently, in the Sun-Earth system, several asteroids have been discovered in horseshoe orbits, including 2010 SO16, 2002 AA29, and 3753 Cruithne (which has high orbital eccentricity and inclination, and so is included in wider classifications of horseshoe orbits) [5]. In the years since, many advancements in the understanding and modelling of such co-orbital motion have occurred, including Christou in 2000 [6], who showed that transitions from tadpole orbits to horseshoe orbits exist since the two regions are connected, and surveys of the population of asteroids in co-orbital motion with solar system bodies [7, 8], amongst others e.g. [9, 10].

A largely unexplored concept, however, is the generation of artificial horseshoe orbits in two-body systems for the purposes of spacecraft formation flight and constellation forming. It can be envisaged that, in the absence of a secondary gravitational body, continuous acceleration due to low thrust propulsion could be used to replicate certain aspects of co-orbital behaviour. With the advent of modern low-thrust, high specific impulse propulsion, such a concept could be readily achievable. The use of continuous thrust to counteract certain components of gravity or centripetal acceleration was first studied by Dusek to create artificial equilibria near three-body Lagrange points [11], and the similar concept of using thrust to displace the plane of an orbit in a two-body system was later researched by several authors [12, 13, 14]. These displaced-plane orbits have been termed non-Keplerian orbits (NKO) since the orbit plane does not intersect the barycentre of the system. Further, the use of solar sails to displace the plane of a geostationary orbit has been studied [15, 16], and a global classification of NKOs was performed by McKay et al. [17]. In 2016, Arnot and McInnes further developed and classified types of low-thrust augmented relative orbits for spacecraft formations [18].

This paper, using the cylindrical-polar form of the Clohessy-Wiltshire equations of motion relative to a circular reference orbit, presents a series of ways in which apparent co-orbital motion can be produced artificially using simple continuous thrust commands. In-plane motion is then combined with free-flying and forced out-of-plane motion (including the implementation of NKOs) to produce phased spacecraft constellations on three-dimensionally nested horseshoe orbits, with respect to an example geostationary reference orbit. The Δv requirements of such orbits are presented and a final discussion of the applicability of the relative orbits and associated constellations is given.

2. Relative motion in the rotating frame

The work presented in this paper is based on the linear reduction of Hill's equations, considering spacecraft motion relative to a circular reference orbit around a central body, known as the Clohessy-Wiltshire (CW) equations. Motion governed by these equations exhibits certain aspects of co-orbital motion [19]. They are given here in the cylindrical coordinates δr, $\delta\theta$, and δz as [20]

$$\delta\ddot{r} = 2nr_0\delta\dot{\theta} + 3n^2\delta r + a_r \tag{1a}$$

$$\delta\ddot{\theta} = \frac{-2n\delta\dot{r} + a_\theta}{r_0} \tag{1b}$$

$$\delta\ddot{z} = -n^2\delta z + a_z \tag{1c}$$

The cylindrical form of the CW equations is used since it is correct for any change in along-track displacement, unlike the Cartesian form. Here, n and r_0 are the mean motion and radius of the reference orbit, and a_r, a_θ, and a_z are the thrust-induced accelerations in the radial, along-track, and out-of-plane directions respectively. Note that, since Eq. (1a) and (1b) are coupled and Eq. (1c) is decoupled from the other two, it is possible to consider the in-plane and out-of-plane motion separately, as will be done later.

The general solutions to Eq. (1a-c) when the input accelerations are zero are given as

$$\delta r(t) = -\left(\frac{2}{n}r_0\delta\dot{\theta}_0 + 3\delta r_0\right)\cos nt + \frac{\delta\dot{r}_0}{n}\sin nt + 4\delta r_0 + \frac{2}{n}r_0\delta\dot{\theta}_0 \tag{2a}$$

$$\delta\theta(t) = \delta\theta_0 - \left(3\delta\dot{\theta}_0 + \frac{6n\delta r_0}{r_0}\right)t + \left(\frac{4\delta\dot{\theta}_0}{n} + \frac{6\delta r_0}{r_0}\right)\sin nt + \frac{2\delta\dot{r}_0}{nr_0}\cos nt - \frac{2\delta\dot{r}_0}{nr_0} \tag{2b}$$

$$\delta z(t) = \delta z_0\cos nt + \frac{\delta\dot{z}_0}{n}\sin nt \tag{2c}$$

2. Transfers using single-axis thrust

It will now be shown that it is possible to achieve artificial horseshoe orbits using only thrust in the along-track direction. This orbit will be comprised of two symmetrical transfer manoeuvres, one to lower the orbit and another to raise it again, connected by two ballistic trajectories. For this, we require both the ballistic solutions given by Eq. (2a-b) and the following solutions for the position with nonzero along-track thrust, given as

$$\delta r(t) = \Big(2n\left(a_\theta t + r_0\delta\dot{\theta}_0 + 2n\delta r_0\right) - n\left(2r_0\delta\dot{\theta}_0 + 3n\delta r_0\right)\cos(nt) + \left(-2a_\theta + n\delta\dot{r}_0\right)\sin(nt)\Big)\Big/n^2 \tag{3a}$$

$$\delta\theta(t) = \frac{1}{2n^2r_0}\Big(a_\theta\left(8-3n^2t^2\right) - 2n\left(2\delta\dot{r}_0 + n\left(3r_0t\delta\dot{\theta}_0 + 6nt\delta r_0 - r_0\delta\theta_0\right)\right) + \left(-8a_\theta + 4n\delta\dot{r}_0\right)\cos(nt) + 4n\left(2r_0\delta\dot{\theta}_0 + 3n\delta r_0\right)\sin(nt)\Big) \tag{3b}$$

If we assume that the initial orbit is circular, then the initial along-track velocity is $\delta\dot{\theta}_0 = -3n\delta r/(2r_0)$. We also establish that the reference orbit period T is given by $T = 2\pi/n$, that the relative orbit completes at $t = 2T$, and that the duration of the thrust arc is given by t_1. To simplify the problem further, we select $\delta\dot{r}_0 = 0$ and $\delta\theta_0 = 0$.

The orbit can now be defined with a piecewise function, expanded as four sets of solutions to the equations of motion using the general solutions of Eq.(2a-b) and Eq. (3a-b) at times $t = \{t_1, t_2, t_3, t_4\}$, each of which gives either the position or velocity of the spacecraft at the end of each powered or unpowered section. Thus, we find expressions for the final state of the system in terms of the initial conditions, the along-track thrust, and the duration of the powered arc. It can be shown that the equations for the final state (denoted by the subscript '4') of the system, having returned to its initial conditions, are given by

$$\delta r_4 = \delta r_0 \tag{4a}$$

$$\delta\theta_4 = -\frac{6\pi(a_\theta t_1 + n\delta r_0)}{nr_0} \tag{4b}$$

$$\delta\dot{r}_4 = 0 \tag{4c}$$

$$\delta\dot{\theta}_4 = -\frac{3n\delta r_0}{2r_0} \tag{4d}$$

Note that Eq. (4b) is the only equation dependent on a_θ and t_1. It is therefore possible to solve it for a_θ. By selecting $\delta\theta_4 = \delta\theta_0$, it is found that

$$a_\theta = -\frac{n\delta r_0}{t_1} \qquad (5)$$

Thus, the required thrust-induced acceleration can be found by selecting the initial radial displacement and the manoeuvre duration.

Using Eq. (5) to define the thrust and by placing the spacecraft into the intended initial circular ballistic orbit, we find that the decelerating powered manoeuvre transfers the spacecraft onto a lower elliptical orbit. After a single orbit period has elapsed, the reverse thrust is applied for duration t_1, and the spacecraft is returned to its initial circular ballistic orbit. At $t = 2T$, the relative orbit is completed and the spacecraft has returned to its initial conditions. The result of a numerical simulation testing this is shown in Fig. 1.

It is also worth noting that, so long as the magnitudes of a_θ and t_1 are kept the same for both the deceleration and acceleration manoeuvres, the result is a repeating orbit of similar shape to the case in Fig. 1. However, as stated, the special property given by Eq. (5) is that the relative orbit completes in exactly two reference orbit periods. Figure 2 illustrates how this property can be extended over any integer multiple of two orbit periods (in this case, 6) to form a longer horseshoe orbit. Figure 3 shows how this kind of orbit maps to the Earth-centred inertial reference frame, with modified dimensions for clarity.

Using the example of an initial radial displacement of 1000 metres above geostationary orbit, as in Fig. 1, the Δv required for one full horseshoe orbit (two symmetrical transfers) is less than 0.15 ms^{-1}. This value scales linearly, and so an initial displacement of 10 km would result in a Δv of under 1.5 ms^{-1}.

So long as the thrust magnitude and duration obey Eq. (5), different initial radial displacements can be selected for a constellation of spacecraft to follow nested horseshoe orbits, all with the same relative orbit period. This could permit interesting new families of phased constellations, the applications of which could be diverse.

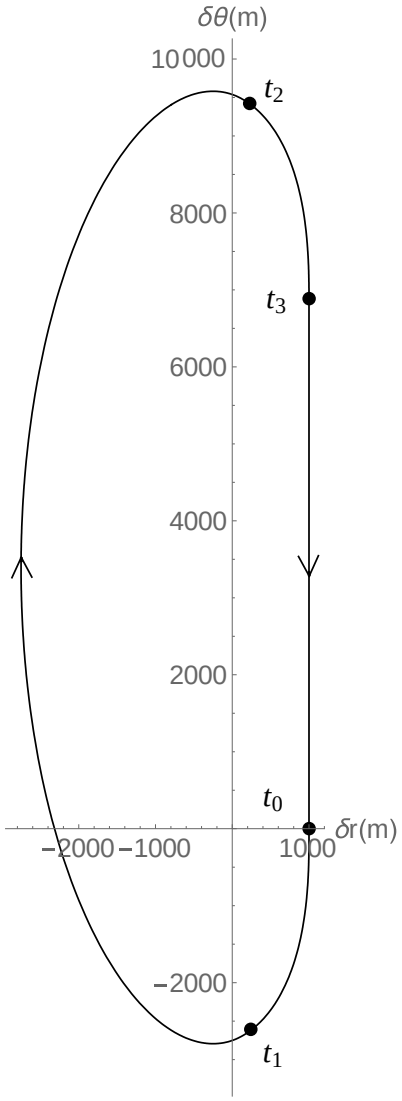

Figure 1. Short horseshoe orbit using single-axis thrust between times t_0 and t_1, t_2 and t_3.

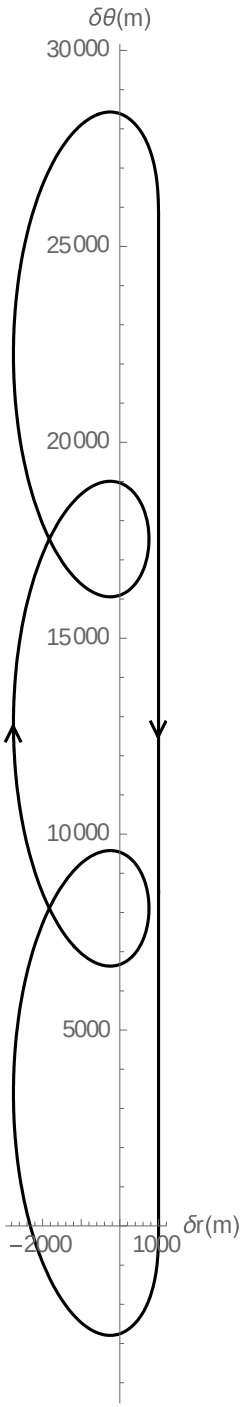

Figure 2. Horseshoe orbit with period of 6*T* using transfers with single-axis thrust.

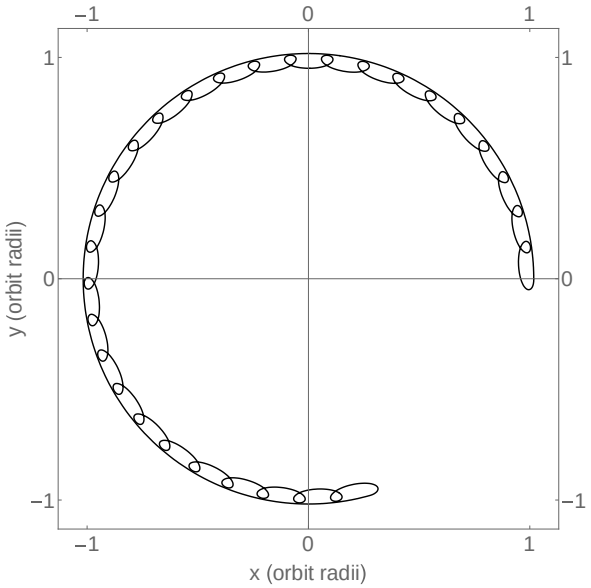

Figure 3. Long horseshoe orbit mapped to the Earth-centred rotating frame, using two transfers with single-axis thrust.

3. Transfers using dual-axis thrust

A geometrically simple and operationally advantageous version of a horseshoe orbit is one which is composed of two circular orbits of different radius, connected by powered transfer trajectories. In such a case, thrust would only be required for the duration of the transfers between the upper and lower circular orbits. It is proposed that this could be achieved using continuous low thrust in two axes (the along-track and radial axes) to at once change the semi-major axis of the spacecraft's orbit and produce the correct conditions at the end of the transfer to induce a resulting ballistic circular orbit.

Normally, bounded relative motion in the rotating frame is elliptical, resulting from the cancellation of the secular term by selecting $\delta\dot{\theta}_0 = -2n\delta r_0 / r_0$. From [18], it can be shown that by using thrust to cancel the second term of Eq. (1a), i.e. $a_r = -3n^2\delta r$, circular in-plane relative motion can be achieved with the same initial conditions as the ballistic elliptical case. With the appropriate initial along-track velocity and radial thrust, the result is a circular relative orbit in the $r-\theta$ plane. This forced circular relative orbit is shown in Fig. 4. Note that the initial velocity for the forced circular relative orbit is not the relative velocity of a spacecraft on a straight-line along-track trajectory in the rotating frame (corresponding to a circular orbit in the inertial frame). As such, this radial thrust command appears to provide a basis for the transfer between two different circular orbits, however work must be done to ensure that the along-track velocity at the beginning and end of the transfer is $\delta\dot{\theta}_0 = \delta\dot{\theta}_1 = -3n\delta r/(2r_0)$.

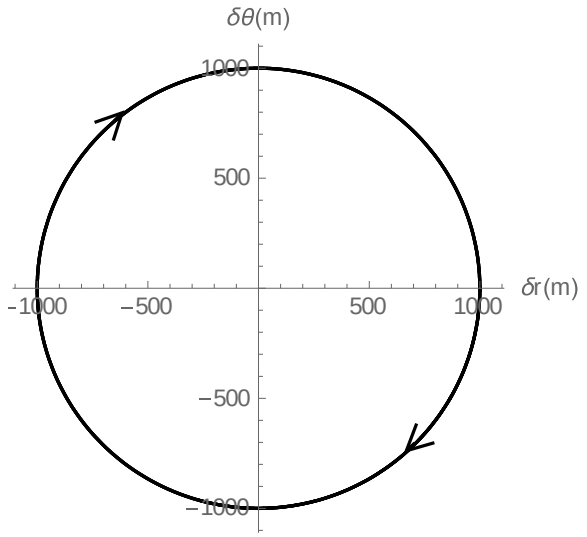

Figure 4. Forced circular relative orbit using radial thrust $a_r = -3n^2\delta r$.

The relative motion exhibited by a spacecraft using the above radial acceleration for an along-track direction reversal is shown in Fig. 5, in which the spacecraft begins at 1000 metres above geostationary orbit with the initial velocity required for a flat trajectory, and has its thrust activated for quarter of an orbit period. This duration corresponds to the time required to return to the initial along-track displacement. As can be seen, at the end of the powered manoeuvre the spacecraft retains an along-track velocity greater than that required for a flat relative trajectory at lower altitude. As such, the spacecraft climbs above and falls behind the reference point. Conceptually, since the post-manoeuvre along-track velocity is greater than that required for an inertial-frame circular orbit, the spacecraft must have a nonzero orbital eccentricity. Thus, it is necessary for the spacecraft to also lose energy during the manoeuvre to attain the correct final orbit.

It is proposed that the simplest way to achieve this is to use a constant along-track thrust induced acceleration. Considering only the in-plane motion since the out-of-plane motion is decoupled, it is first necessary to find the general solutions to Eq. (1a) and (1b) when $a_r = -3n^2\delta r$ and a_θ is a constant. Proceeding, the general solutions are found as

$$\delta r(t) = -\Big(-2n\left(2\delta r_0 n + a_\theta t + r_0\delta\dot{\theta}_0\right) + 2nr_0\delta\dot{\theta}_0\cos(2nt) + \left(a_\theta - 2n\delta\dot{r}_0\right)\sin(2nt)\Big)\Big/\left(4n^2\right) \tag{6a}$$

$$\delta\theta(t) = \Big(a_\theta + 4\delta\theta_0 n^2 r_0 - 2n\delta\dot{r}_o - \left(a_\theta - 2n\delta\dot{r}_o\right)\cos(2nt) + 2nr_0\delta\dot{\theta}_0\sin(2nt)\Big)\Big/\left(4n^2 r_0\right) \tag{6b}$$

Taking the derivative yields the general solution for the velocity as

$$\delta\dot{r}(t) = \frac{a_\theta - \left(a_\theta - 2n\delta\dot{r}_0\right)\cos(2nt) + 2nr_0\delta\dot{\theta}_0\sin(2nt)}{2n} \tag{7a}$$

$$\delta\dot{\theta}(t) = \delta\dot{\theta}_0\cos(2nt) + \frac{\left(a_\theta - 2n\delta\dot{r}_0\right)\sin(2nt)}{2nr_0} \tag{7b}$$

Then it is necessary to define the required initial and final conditions of the manoeuvre. Assuming the manoeuvre takes place at the crossing of the δr axis, and that the manoeuvre ends when the spacecraft re-crosses the same axis, we have $\delta\theta_0 = \delta\theta_1 = 0$ where the subscript "1" denotes the final condition at time t. Since the initial orbit and final orbits must be circular (with flat trajectory in the rotating frame), we must have $\delta\dot{\theta}_0 = \delta\dot{\theta}_1 = -3n\delta r/(2r_0)$. Substituting $\delta r_1 = -\delta r_0$ into Eq. (6a) and $\delta\dot{r}_0 = 0$ into Eq. (7a) and rearranging for a_θ in each case yields two different expressions for the required thrust induced acceleration. These are

$$a_\theta = \frac{2n\left(\delta r_0\cos(2nt) + r_0\delta\dot{\theta}_0\sin(2nt)\right)}{-1+\cos(2nt)} \tag{8a}$$

$$a_\theta = -\frac{2n\left(r_0\delta\dot{\theta}_0 + 4n\delta r_0 - r_0\delta\dot{\theta}_0\cos(2nt) + \delta\dot{r}_0\sin(2nt)\right)}{2nt - \sin(2nt)} \tag{8b}$$

Finding the intersection of Eq. (8a) and (8b) yields the duration of the manoeuvre, ending at time t_1. Once the value t_1 is known, it can be substituted into either equation to find the required thrust induced acceleration. It should also be noted that, in this case, the time t_1 is dependent only on the natural dynamics of the system and not the initial displacement of the spacecraft. Therefore, a manoeuvre beginning at any initial radial position will complete in the same time. This is demonstrated in Fig. 6, where the transfer manoeuvre is performed for three circular initial orbits of different radius. Note that by performing the reverse manoeuvre, the relative orbit track can be repeated. Also, the time before the reverse manoeuvre is entirely arbitrary, and so the horseshoe orbit could be extended around the

entirety of the reference orbit. Figure 7 illustrates how such an artificial horseshoe orbit maps to the Earth-centred rotating frame, with the radial dimensions modified for clarity.

For a single complete horseshoe orbit using this type of transfer (assuming independent face-mounted axis-aligned thrusters), for an initial radial displacement of 1000 m the total required Δv is 0.64 ms^{-1}, of which approximately 0.5 ms^{-1} is from the radial component. This expenditure scales linearly with initial radial displacement: as before, 10 km initial displacement would result in a Δv of 6.4 ms^{-1} for a full horseshoe orbit.

It is clear from the figures that this type of orbit provides great potential utility, since the transfers are geometrically simple and the initial and final orbits are both circular. The ability to arbitrarily select the point at which a reverse manoeuvre is performed adds great versatility to this type of trajectory, thanks to the uniform along-track velocity and radial displacement offered by the circular orbits.

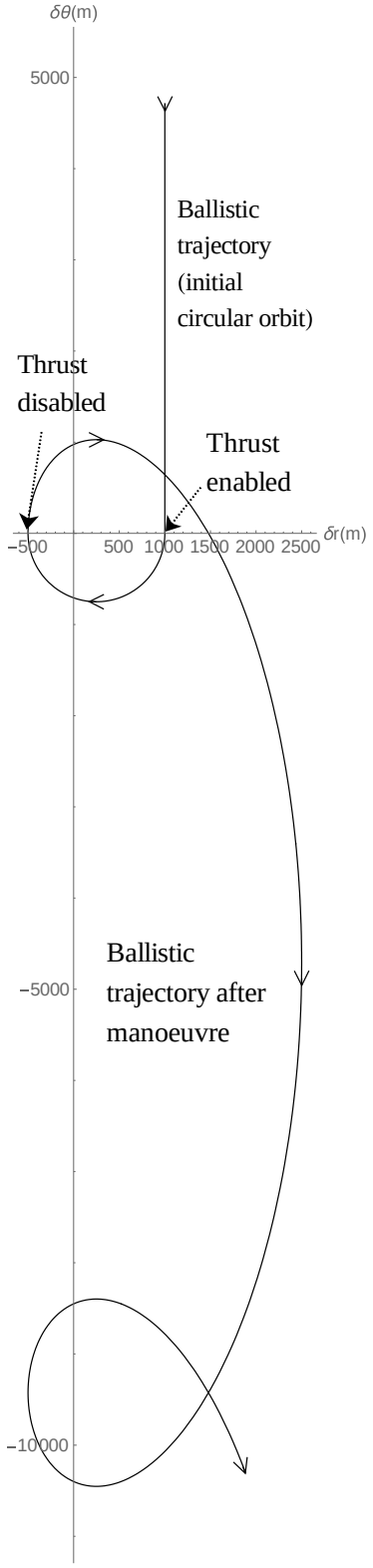

Figure 5. Ballistic trajectory following a radial thrust manoeuvre.

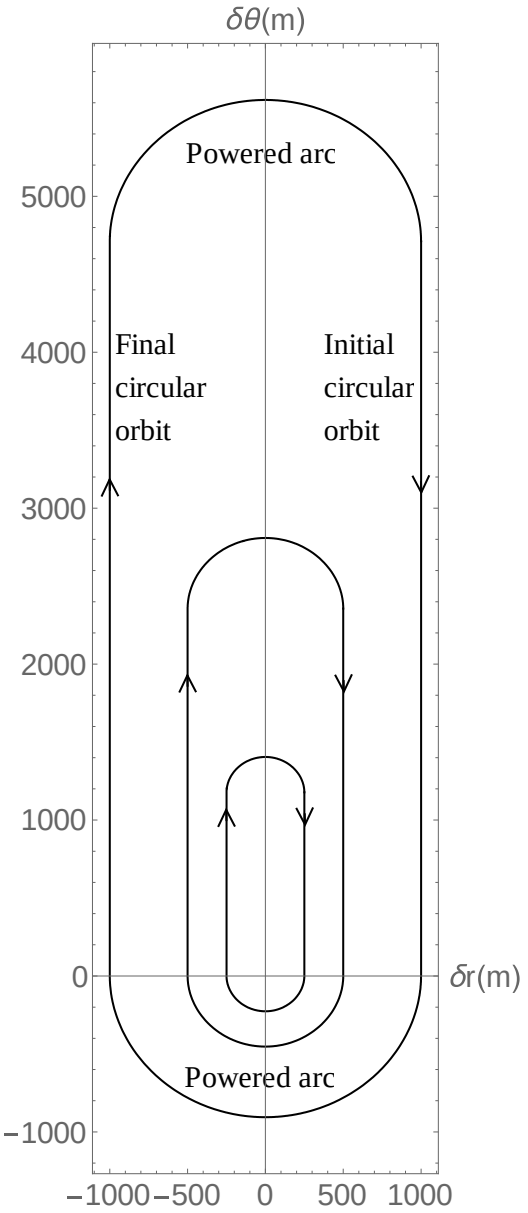

Figure 6. Nested horseshoe orbits using transfers with dual-axis thrust.

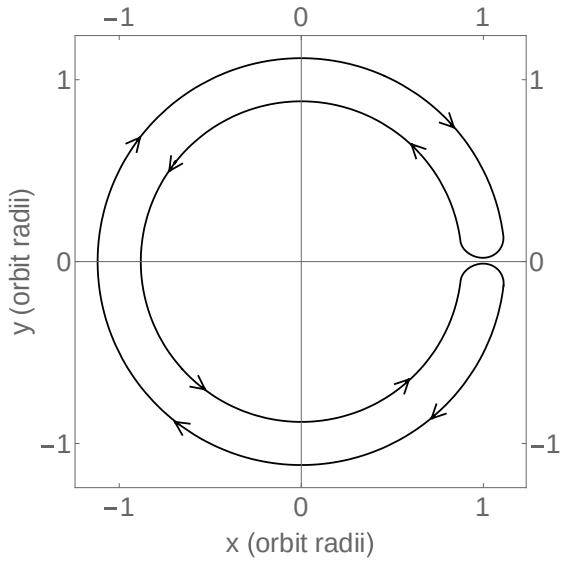

Figure 7. Artificial horseshoe orbit with exaggerated radial dimensions in Earth-centred rotating frame.

4. Three-axis motion

Now that two different methods for generating artificial horseshoe orbits have been established, but considering only the in-plane motion, it is now proposed to introduce out-of-plane motion. Adding another dimension to the motion also adds to the ways in which nested horseshoes orbits can be implemented. Since the out-of-plane motion is decoupled from the in-plane motion, it can be developed entirely separately. In the Earth-centred inertial frame, out-of-plane displacements correspond to a nonzero relative inclination between the orbit and the reference orbit.

With zero input thrust and nonzero initial out-of-plane displacement, the δz -axis motion is that of a simple harmonic oscillator which cycles with a period of $T_z = 2\pi/n$. Combined with the artificial in-plane horseshoe motion, even this simple ballistic case generates interesting trajectories, as shown in Fig. 8 and Fig. 9. Figure 10 and Fig. 11 show the 3D trajectories when using transfers with dual-axis thrust. However, greater variety and versatility can be found when continuous thrust is used to modify the frequency of the out-of-plane motion.

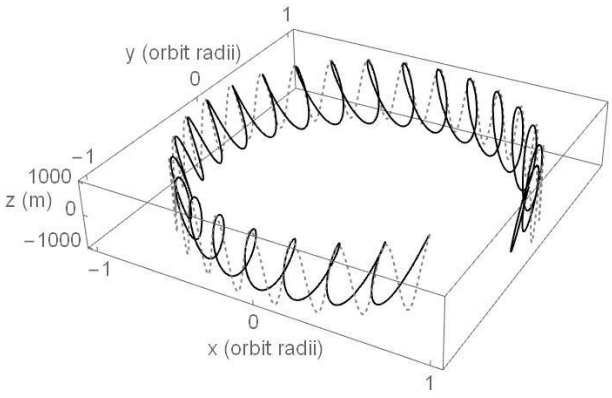

Figure 8. Artificial horseshoe orbit in the Earth-centred rotating frame using two single-axis thrust transfers and nonzero δz -axis displacement. The solid black line is the elliptical section and the dashed grey line is the circular final orbit. Radial dimensions have been exaggerated for clarity.

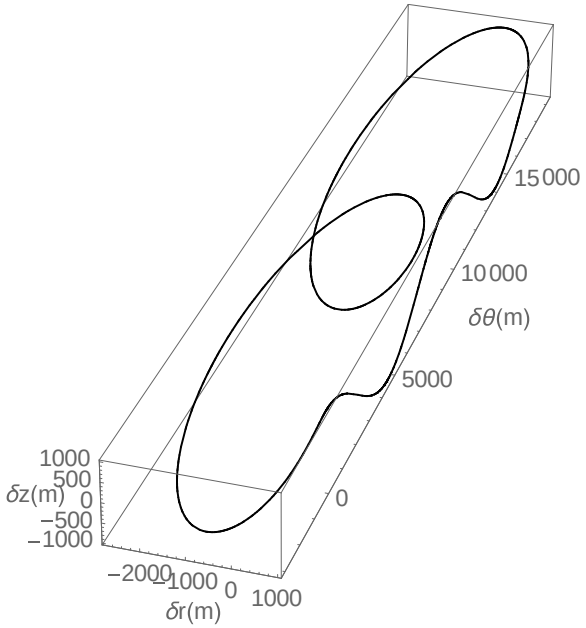

Figure 9. Short artificial horseshoe orbit using transfers with single-axis thrust and nonzero δz -axis displacement.

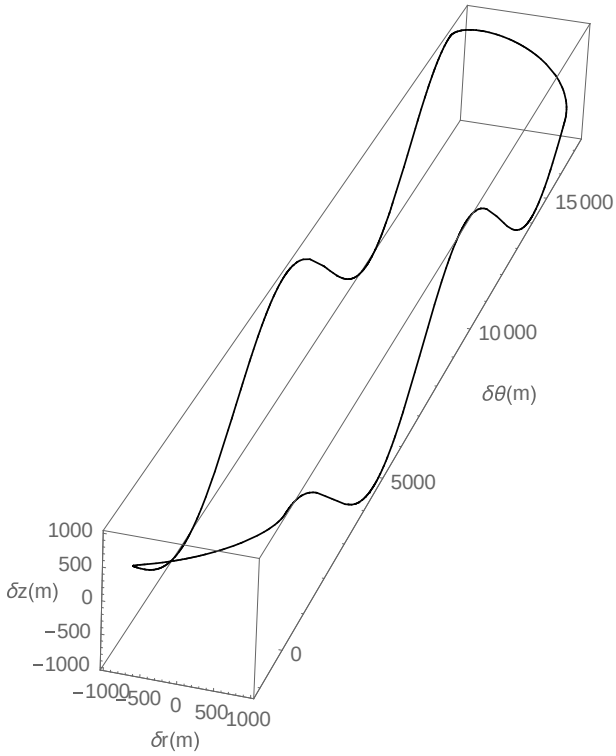

Figure 10. Short artificial horseshoe orbit using transfers with dual-axis thrust and nonzero δz -axis displacement.

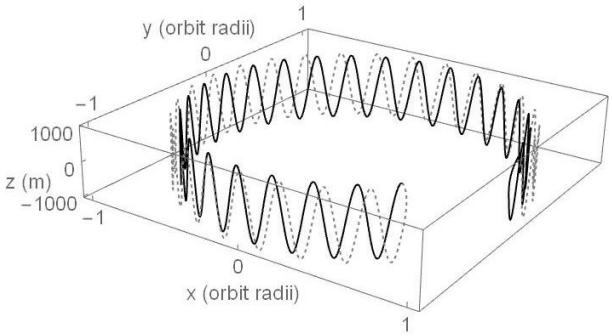

Figure 11. Artificial horseshoe orbit in the Earth-centred rotating frame using transfers with dual-axis thrust and nonzero δz -axis displacement. The solid black line is circular initial orbit, and the dashed grey line is circular final orbit. Radial dimensions have been exaggerated for clarity.

Referring to Arnot and McInnes [18], it is possible to change the natural frequency of the out-of-plane motion by making the thrust input proportional to out-of-plane displacement. Using this framework, the case of a statically displaced NKO [14] can be considered a relative orbit with infinite period along the δz -axis.

Considering Eq. (1c), we make the input acceleration proportional to δz by selecting

$$a_z = \lambda^2 \delta z \tag{9}$$

in which λ is the modified mean motion. It can be shown that, in order to change the period of the out-of-plane motion by a factor k, such that $T_z=kT$, we have

$$\lambda = n\sqrt{1-\left(\frac{1}{k^2}\right)} \tag{10}$$

This substitutes into Eq. (9) to give

$$a_z = n^2 \delta z\left(1-\frac{1}{k^2}\right) \tag{11}$$

The out-of-plane motion is now given by the augmented equation

$$\delta \ddot{z} = -\frac{n^2 \delta z}{k^2} \tag{12}$$

This augmented out-of-plane motion is exhibited in Fig. 12 and Fig. 13, where the out-of-plane motion clearly has a different period to that of the in-plane motion. Further, when $a_z = n^2 \delta z$ (i.e. $k \to \infty$), the result is a statically displaced NKO. To maintain such a NKO at 1000 m displacement out-of-plane from geostationary orbit requires Δv of approximately 168 ms^{-1} per year. Though this seems to be a high figure, for a 10 kg microsatellite equipped with electrostatic ion thrusters (assuming a specific impulse of 3000 s), this equates to a modest propellant expenditure of only 0.057 kg. According to Eq. (11), it is clear that all other cases require lower acceleration magnitudes and therefore lower Δv.

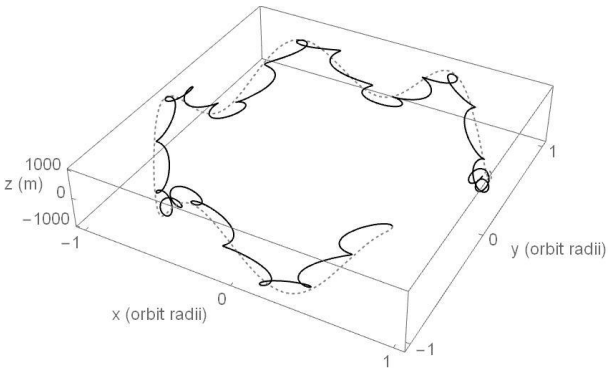

Figure 12. Horseshoe orbit with single-axis thrust transfers and thrust augmented out-of-plane motion ($T_z=5T$). Solid black line is circular initial orbit, and dashed grey line is circular final orbit. Radial dimensions have been exaggerated for clarity.

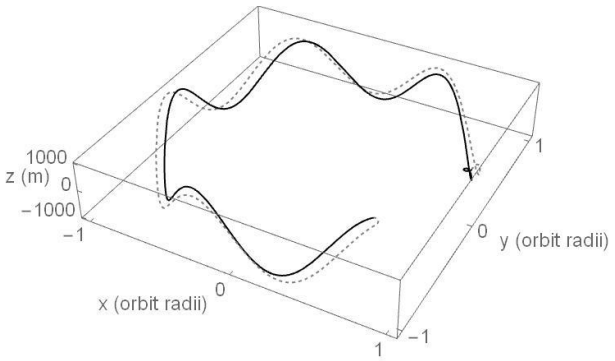

Figure 13. Horseshoe orbit with dual-axis thrust transfers and thrust augmented out-of-plane motion ($T_z=5T$). Solid black line is circular initial orbit, and dashed grey line is circular final orbit. Radial dimensions have been exaggerated for clarity.

5. Discussion

The two methods proposed for generating artificial horseshoe orbits both offer the possibility of creating constellations of spacecraft on nested relative orbits. The simplest and arguably most versatile of the two horseshoe orbits is the dual-axis thrust version described in Section 3. Taking this as an example, it would be possible to nest several of these horseshoe orbits inside one another by giving each spacecraft a different initial displacement. Each of these spacecraft would have a different relative velocity, but assuming that the transfer manoeuvres are performed at the same time, their motion would remain synchronised since the duration of the manoeuvre t_1 is the same for all radial displacements. Phased motion can be introduced by varying the initial along-track displacement of the spacecraft. Additionally, by using augmented out-of-plane motion, nested horseshoe orbits can be fixed in different planes or with different out-of-plane frequency to produce even more rich new families of relative orbits. Figure 14 shows an example configuration in which three spacecraft follow identical horseshoe orbits which are separated by phase.

The circularity of both inner and outer orbits of the horseshoe with dual-axis thrust transfers offers potentially great operational versatility. It can be envisaged that constellations of small satellites following such nested, phased, and displaced-plane orbits could be designed for a wide range of applications including on-orbit inspection, disaggregated spacecraft, and hyperspectral sensing. Furthermore, reconfigurable constellations could be developed which allow, in the geostationary ring example, concentration of spacecraft over certain longitudes at required times, building upon the concepts of McInnes, and Mushet et al. [21, 22].

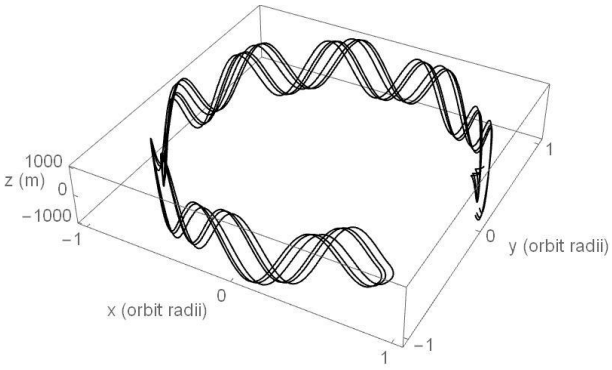

Figure 14. Three phased horseshoe orbits with dual-axis thrust transfers and thrust augmented out-of-plane motion (T_z=3T), and different δz_0. Radial dimensions have been exaggerated for clarity.

6. Conclusions

It has been shown that certain aspects of co-orbital relative motion in three-body systems can be replicated in a linear two-body system with the addition of low thrust. Using simple thrust commands, transfers between ballistic orbits have been developed to generate artificial horseshoe orbits. For small Δv, horseshoe orbits of arbitrary length can be generated, and synchronised nested orbits can be achieved since the transfer manoeuvre duration is constant and independent of radial displacement. It has also been shown that non-Keplerian horseshoe orbits using out-of-plane thrust are achievable, providing access to another rich new family of relative orbits.

Acknowledgements

This research was supported by an Engineering and Physical Sciences Research Council (EPSRC) Doctoral Training Grant (CSA), and a Royal Society Wolfson Research Merit Award (CRM).

References

[1] E.C. Stone, E.D. Miner, Voyager 1 Encounter with the Saturnian System, Science, New Series, Vol. 212, No. 4491 (1981) 159–163.

[2] B.A. Smith, Voyager Imaging Team, Encounter with Saturn: Voyager 1 Imaging Science Results, Science, New Series, Vol. 212, No. 4491 (1981) 163-191.

[3] S.P. Synnott, C.F. Peters, B.A. Smith, L.A. Morabito, Orbits of the Small Satellites of Saturn, Science, New Series, Vol. 212, No, 4491 (1981) 191–192.

[4] B. Garfinkel, Theory of the Trojan asteroids, Astron. J., Vol. 82 No. 5 (1977) 368–379.

[5] U. Walter, Astronautics: The Physics of Spaceflight, second ed., Wiley-VCH, Weinheim, Germany, (2012) 405.

[6] A.A. Christou, A Numerical Survey of Transient Co-orbitals of the Terrestrial Planets, Icarus, Vol. 144 (2000) 1-20.

[7] M.H.M. Morais, A. Morbidelli, The Population of Near-Earth Asteroids in Coorbital Motion with the Earth, Icarus, Vol. 160, (2002) 1-9.

[8] M.H.M. Morais, A. Morbidelli, The Population of Near Earth Asteroids in Coorbital Motion with Venus, Icarus, Vol. 185 (2006) 29-38.

[9] P. Robutel, A. Pousse, On the co-orbital motion of two planets in quasi-circular orbits, Celestial Mechanics and Dynamical Astronomy, Vol. 117 (2013) 17-40.

[10] C.A. Giuppone, C. Beaugé, T.A. Michtchenko, S. Ferraz-Mello, Dynamics of two planets in co-orbital motion, Monthly Notices of the Royal Astronomical Society, Vol. 407, No. 1, (2010) 390-398.

[11] H.M. Dusek, Motion in the vicinity of libration points of a generalized restricted three-body model, Progress in Astronautics and Aeronautics, Vol. 17, (1966) 743-759.

[12] K.T. Nock, Rendezvous with Saturn's rings, Planetary rings: 1st international meeting, CNES, Toulouse, France, (1984) 743-759

[13] G.J. Yashko, D.E. Hastings, Analysis of thruster requirements and capabilities for local satellite clusters, 10th AIAA/USU Conference on Small Satellites, AIAA, Logan, Utah, (1996)

[14] C.R. McInnes, The existence and stability of families of displaced two-body orbits, Celestial Mechanics and Dynamical Astronomy, Vol. 67, No. 2, (1997) 167-180
doi: 10.1023/A:1008280609889

[15] S. Baig, C.R. McInnes, Artificial three-body equilibria for hybrid low-thrust propulsion, Journal of Guidance, Control, and Dynamics, Vol. 31, No. 2, (2008) 1644-1655
doi: 10.2514/1.36125

[16] J. Heiligers, C.R. McInnes, J.D. Biggs, M. Ceriotti, Displaced geostationary orbits using hybrid low-thrust propulsion, Acta Astronautica, Vol. 71, (2012) 51-67
doi: 10.1016/j.actaastro.2011.08.012

[17] R.J. McKay, M. Macdonald, J. Biggs, C.R. McInnes, Survey of highly non-Keplerian orbits with low-thrust propulsion, Journal of Guidance, Control, and Dynamics, Vol. 34, No. 3, (2011) 645-666 doi: 10.2514/1.52133

[18] C.S. Arnot, C.R. McInnes, Low thrust augmented spacecraft formation-flying for on-orbit inspection, IAC-15-C1.8.1, 66th International Astronautical Congress, Jerusalem, Israel, 2015, 12 – 16 October.

[19] R. Broucke, A.E. Roy (ed.), Some models for the motion of co-orbital satellites of Saturn, Long-Term Dynamical Behaviour of Natural and Artificial N-Body Systems, Part II, Springer, (1988) 155-169.

[20] W.E. Wiesel, Spaceflight Dynamics, second ed., McGraw-Hill, Singapore, (1997) 80-81.

[21] C.R. McInnes, Autonomous ring formation for a planar constellation of satellites, Journal of Guidance, Control, and Dynamics, Vol. 18, No. 5, (1995) 1215-1217.

[22] G.S. Mushet, G. Mignotti, C. Colombo, C.R. McInnes, Self-organizing Satellite Constellation in Geostationary Earth Orbit, IEEE Transactions on Aerospace and Electronic Systems, Vol. 51, No. 2, (2015) 910-923.
doi: 10.1109/TAES.2014.130690